

Role of sphingolipids in the transport of prosaposin to the lysosomes

Stephane Lefrancois,* Lorraine Michaud,† Michel Potier,† Suleiman Igdoura,§
and Carlos R. Morales^{1,*}

Department of Anatomy and Cell Biology,* McGill University; Centre de Recherche,† Hôpital Sainte-Justine, Université de Montréal; and Department of Human Genetics,§ Montreal Children's Hospital, Montreal, Quebec, Canada

Abstract Prosaposin is the precursor of four lysosomal saposins that promote the degradation of glycosphingolipids (GSLs) by acidic hydrolases. GSLs contain a hydrophobic ceramide moiety, which acts as a membrane anchor, and a hydrophilic oligosaccharide chain that faces the lumen of the Golgi apparatus and extracellular spaces. By using fumonisin B1, PDMP and D609, we tested the hypothesis that sphingolipids mediate the transport of prosaposin to the lysosomes. Fumonisin B1 interferes with the synthesis of ceramide, PDMP blocks the formation of glucosylceramide and D609 blocks the formation of sphingomyelin. Fumonisin B1 produced a 59–85% decrease in the density of gold particles in the lysosomes of CHO and NRK cells immunolabeled with anti-prosaposin antibody, and a 55% reduction in the lysosomes of CHO cells stably transfected with an expression vector containing a human prosaposin cDNA. To examine whether the mannose 6-phosphate receptor pathway was affected by this treatment, NRK and CHO cells treated or not with fumonisin B1 were labeled with anti-cathepsin A antibody. The results showed no significant differences in labeling of the lysosomes, suggesting that the effect of fumonisin B1 was specific. When fumonisin B1 and D609 were added to the media of transfected CHO cells, a decrease in immunofluorescence with anti-prosaposin antibody was observed by confocal microscopy. PDMP did not cause any reduction in immunoreactivity, indicating that sphingomyelin appears to be involved in this process. **In conclusion, our data support the hypothesis that sphingolipids, possibly sphingomyelin, are involved in the transport of prosaposin to the lysosomes.**—Lefrancois, S., L. Michaud, M. Potier, S. Igdoura, and C. R. Morales. **Role of sphingolipids in the transport of prosaposin to the lysosomes.** *J. Lipid Res.* 1999. 40: 1593–1603.

Supplementary key words prosaposin • saposins • sphingolipids • lysosomal transport • fumonisin B1 • PDMP • D609

Prosaposin is the precursor of four nonenzymic lysosomal proteins that are essential cofactors for the degradation of most glycosphingolipids (GSLs) with short oligosaccharide chains by acidic hydrolases (1). GSLs are components of the plasma and Golgi membranes of eu-

karyotic cells. GSLs contain a hydrophobic ceramide moiety, which acts as a membrane anchor, and a hydrophilic oligosaccharide chain, that faces the lumen of the Golgi apparatus and extracellular spaces (1). An in vitro study using recombinant and native prosaposin revealed that this protein combines with GSLs (2). However, detailed studies on the mechanism of transport of prosaposin to the lysosomes are still missing.

The trafficking of lysosomal proteins involves a direct pathway from the Golgi apparatus via the mannose 6-phosphate (M6P) receptor (3) and an indirect pathway from the Golgi apparatus to the plasma membrane and then to the lysosomes via endocytosis (4–6).

According to the first model, lysosomal hydrolases acquire a large pre-formed oligosaccharide side chain within the endoplasmic reticulum (3). These proteins are then transported to the Golgi apparatus where they are tagged with the M6P recognition signal and translocated to the lysosomes (7–11).

According to the second model, membrane-associated lysosomal proteins are transported to the plasma membrane and subsequently reach the lysosomes by endocytic membrane flow (4–6). Proteins that are delivered to the lysosomal compartment by this mechanism display certain characteristics. These proteins have a high number of N-linked sialylated oligosaccharides on their luminal domain, a single membrane-spanning domain and a short C-terminal tail of about 10 or more amino acid residues extending in the cytoplasm (5). Lysosomal acid phosphatase (LAP) which shares many of these characteristics has 7 or 8 N-linked oligosaccharides, a single *trans*-membrane do-

Abbreviations: GLS, glycosphingolipid; M6P, mannose 6-phosphate; CHO, Chinese hamster ovary cells; NRK, normal rat kidney cells; LAP, lysosomal acid phosphatase; Lamp-1, lysosomal associated membrane protein-1; LEP100, lysosomal endosomal protein 100; LIMP-II, lysosomal integral membrane protein-II; PDMP, dl-threo-1-phenyl-2-decanoyl-amino-3-morpholino-1-propanol-HCL; D609, tricyclodecan-9-yl xanthate potassium.

¹ To whom correspondence should be addressed.

main, and a cytoplasmic tail of 18 amino acids (12, 13). LAP is transported from the trans-Golgi elements to the plasma membrane and then is recycled between the plasma membrane and endosomes for several hours (5). This recycling pattern appears to be mediated by a tyrosine residue at position 413 (14). This tyrosine residue has previously been shown to play a role in the internalization of proteins via clathrin-coated endocytic vesicles (15, 16). Finally, after approximately 6 h, LAP is transferred to lysosomes where it becomes trapped. The targeting of LAP to the lysosomal compartment is not affected by M6P processing nor by treatment with weak bases which interfere with lysosomal formation. Other lysosomal proteins that follow this pathway include Lamp-1 (4) and LEP100 (6). A second signal does exist in the lysosomal integral membrane protein-II (LIMP-II). This signal sequence involves a leucine motif that sorts this protein to the plasma membrane and then to the lysosomal compartment (17). LIMP-II is involved in protecting the lysosomal membrane from catabolic breakdown (17).

Prosaposin is not a lysosomal integral membrane protein. Moreover, experimental evidence indicates that prosaposin is targeted to the lysosome by a M6P independent mechanism (18–21). Furthermore, cultured human fibroblasts from human patients with I-cell disease show near normal levels of prosaposin in the lysosomes (22).

In the present study we tested the hypothesis that prosaposin is transported from the Golgi apparatus to the lysosomes bound to sphingolipids anchored to the membrane of cargo vesicles. We tested this hypothesis by inhibiting the synthesis of sphingolipids with fumonisin B1, a fungal metabolite that blocks the formation of ceramide, and the compounds PDMP and D609, which inhibit the synthesis of glucosyl-ceramide and sphingomyelin, respectively.

MATERIAL AND METHODS

Cell lines

Chinese hamster ovary (CHO) cells and CHO cells stably transfected with an expression vector P91023(B) were cultured in F12 COON'S medium (Gibco, Montreal, Quebec) supplemented with 10% fetal calf serum. Normal rat kidney (NRK) cells were provided by Dr. D. Laird (Department of Anatomy and Cell Biology, University of Western Ontario, Canada) and grown in F12 medium supplemented with 10% fetal calf serum. (Gibco, Montreal, Quebec).

Construction of expression vector

Cultured CHO cells do not normally synthesize large amounts of prosaposin. In view of this we used an expression vector to establish a stably transfected CHO cell line that overexpressed human prosaposin. The expression vector P91023 (B) (23) was kindly provided by Dr. R. J. Kaufman (Genetic Institute, Cambridge). A prosaposin cDNA containing a 9 bp insertion of exon 8 (24, 25), was cloned into the EcoRI site of the vector.

Transfection of CHO cells and selection of stably transformed cells

CHO cells ($1-4 \times 10^6$ cells) were seeded on 100-mm dishes 16 h prior to the addition of DNA. Transfection was conducted

using calcium phosphate with 15 μg of DNA. After 72 h in culture, the cells were trypsinized and transferred into 100-mm dishes and selected in a minimum essential medium devoid of nucleosides with 10% dialyzed fetal serum. The resistant colonies were put into culture medium containing 0.02 μM methotrexate. The concentration of methotrexate was progressively increased up to a level of 1 μM . The selected cell lines were analyzed for expression of prosaposin mRNA and its translation product.

Northern blotting

For Northern blot analysis, the mRNA from transformed CHO cells grown in T-150 culture flasks was purified by CsCl gradient centrifugation and resolved by agarose gel electrophoresis (26). The prosaposin cDNA was labeled with the DIG luminescent detection kit of Boehringer Mannheim (Laval, Quebec, Canada), and probed according to the manufacturer specifications.

Immunoprecipitation of prosaposin

Subconfluent transformed CHO cells stably expressing human prosaposin in T-75 flasks were incubated for 1 h in methionine-free medium and labeled for 1 h with [^{35}S]methionine at 0.2 mCi/flask. The cells were washed twice with phosphate-buffered saline and solubilized in 1 ml of 50 mM Tris-HCl (pH 8.0) containing 0.15 M NaCl, 0.5% NP-40, and 10 $\mu\text{g}/\text{ml}$ PMSE.

The cell extract was then precleared by incubation with 50 μl preimmune rabbit serum for 1 h and 500 μl of 10% *S. aureus* polysaccharides was added. After centrifugation, the supernatant was incubated with an antiserum against rat prosaposin overnight at 4°C with shaking. The immune complex was precipitated by the addition of 50 μl of *Staphylococcus aureus* suspension. The antigen-antibody complex was denatured by boiling in the SDS-PAGE loading buffer for 5 min and was analyzed by gel electrophoresis using a 10% gel according to the method of Laemmli (27). The gels were subsequently impregnated with Amplify (Amersham) and the autoradiographs of dried gels were obtained on a X-ray film at -80°C with two intensifying screens during 5 days.

Immunoblotting

Culture media from confluent transformed CHO cells (6 ml) treated or not with fumonisin B1 were collected and concentrated. Previously, 300 μl of 1% Non-idet, 1 mg of aprotinin B, and 2 mg of trypsin inhibitor in 3 ml of buffer phosphate were added to the media. The concentrated media were denatured in 2 \times sample buffer (0.625 M Tris/HCl, pH 6.8, 20% glycerol, 50 mM dithiothreitol, 3% SDS, and 0.001 bromophenol blue) by heating at 100°C, and then electrophoresed on SDS gradient polyacrylamide gel (8–18%) according to Laemmli (27). Proteins were transferred from the unfixed gel onto a nitrocellulose sheet. The nitrocellulose was blocked with 20% goat serum in TBS, incubated with the anti-prosaposin antibody (1:100), and then with alkaline phosphatase-conjugated goat anti-rabbit IgG (1:1000) (28). The blot was then developed using nitro blue tetrazolium and 5-bromo-4-chloro-3-indolyl phosphate as substrates. Quantitative interpretation of the results was carried out by assessing the relative density of bands by densitometric scanning of each band. In all cases three scans were made of each band and averaged to obtain accurate results. A Zeineh Soft Lazer Scanning Densitometer (Biomed Instruments Inc., Chicago, IL) was used for the measurements.

Treatment with inhibitors

For electron microscopy, fumonisin B1 (1 mg) was dissolved in 400 μl of dimethyl sulfoxide (DMSO) and added to the culture

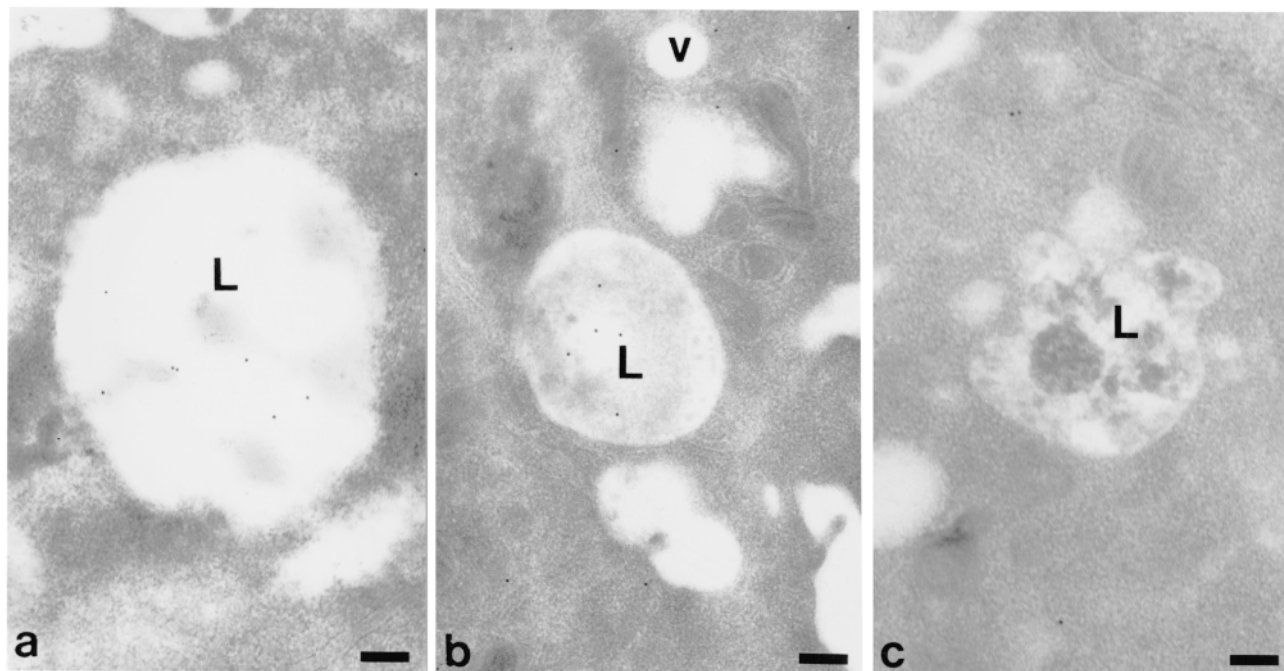


Fig. 1. a) CHO cell (clone 66) cell labeled with anti-cathepsin L antibody. The labeling is seen over a large membrane-bound structure (L) of approximately $0.3 \mu\text{m}$ in diameter; $\times 40,000$; bar = 100 nm . b) NRK cell incubated in control media without fumonisins B1 for 48 h. Notice lysosomes (L) moderately labeled with anti-prosaposin antibody; (v), small vesicle; $\times 35,000$; bar = 150 nm . c) NRK cell incubated in media containing fumonisins B1 for 48 h. Notice lysosome (L) weakly labeled with anti-prosaposin antibody; $\times 35,000$; bar = 150 nm .

media at a concentration of $25 \mu\text{g/ml}$. Duplicate plates of cultured cells were prepared for each experiment in $60 \times 15 \text{ mm}$ Petri dishes. Each dish received 6 ml of media. Half of them contained fumonisins B1 in the medium and the other half received only the fresh media with DMSO. In both cases the cells were incubated for 48 h.

Culture cells were detached from the culture dishes with 0.1% (w/v) trypsin in HBSS (Hank's Balanced Salt Solution). The cells were pelleted at $1000 g$ during 7 min and the supernatant was discarded. The cell pellets were carefully detached from the centrifuge tubes with a needle and fixed in 4% paraformaldehyde and 0.5% glutaraldehyde in 0.05 M phosphate buffer. The cell pellets were dehydrated in methanol and embedded in Lowicryl K11M as described previously by Sylvester et al. (29) and Hermo et al. (30).

For confocal microscopy, CHO 66 cells were grown on coverslips overnight in COON's F12 medium and separated into four groups. Three groups were treated with fumonisins B1 ($25 \mu\text{g/ml}$), PDMP ($25 \mu\text{g/ml}$), D609 ($100 \mu\text{g/ml}$) for 48 h. The fourth

group served as a control. After the 48 h incubation, the cells were washed in PBS for 5 min and then fixed in 3.8% paraformaldehyde for 1 h. The cell membranes were perforated with Triton X-100 and immunostained overnight with anti-prosaposin antibody at a concentration of 1:200. The cells were then washed 3 times, for a period of 10 min each, in PBS containing 0.1% Tween 20 followed by a 1 h incubation with FITC-conjugated anti-rabbit IgG (Sigma-Aldrich, Oakville, Ont.) at a concentration of 1:200. The cells were then washed 3 times, 10 min each time, in PBS containing 0.1% Tween 20 and mounted onto slides using a SlowFade light Antifade kit (Molecular Probes, Eugene, Oregon). The cells were then examined on a Carl Zeiss Confocal microscope.

Immunogold labeling

Ultrathin Lowicryl sections were mounted on 300-mesh Formvar (Polysciences, Inc., Warrington, PA)-coated nickel grids. Each section was then floated for 15 min on a drop of 20 mM

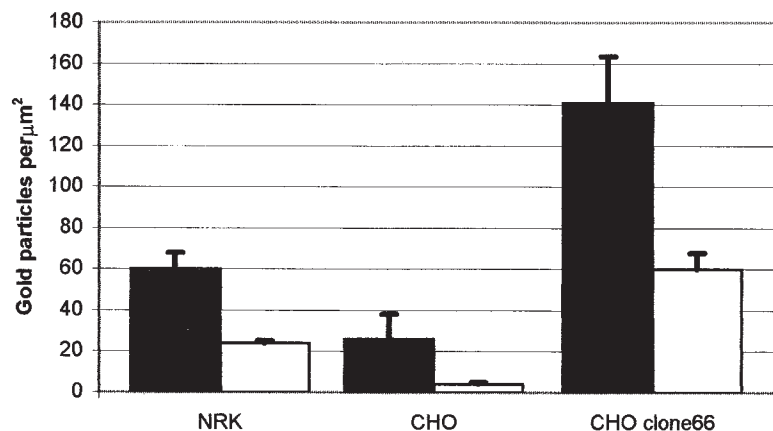


Fig. 2. Bar graph showing the number of colloidal gold particles per μm^2 of lysosome of three cell lines treated (white bars) or not (black bars) with fumonisins B1. NRK and CHO cells were immunoreacted with anti-prosaposin antibody. Error bars represent standard deviation of the mean.

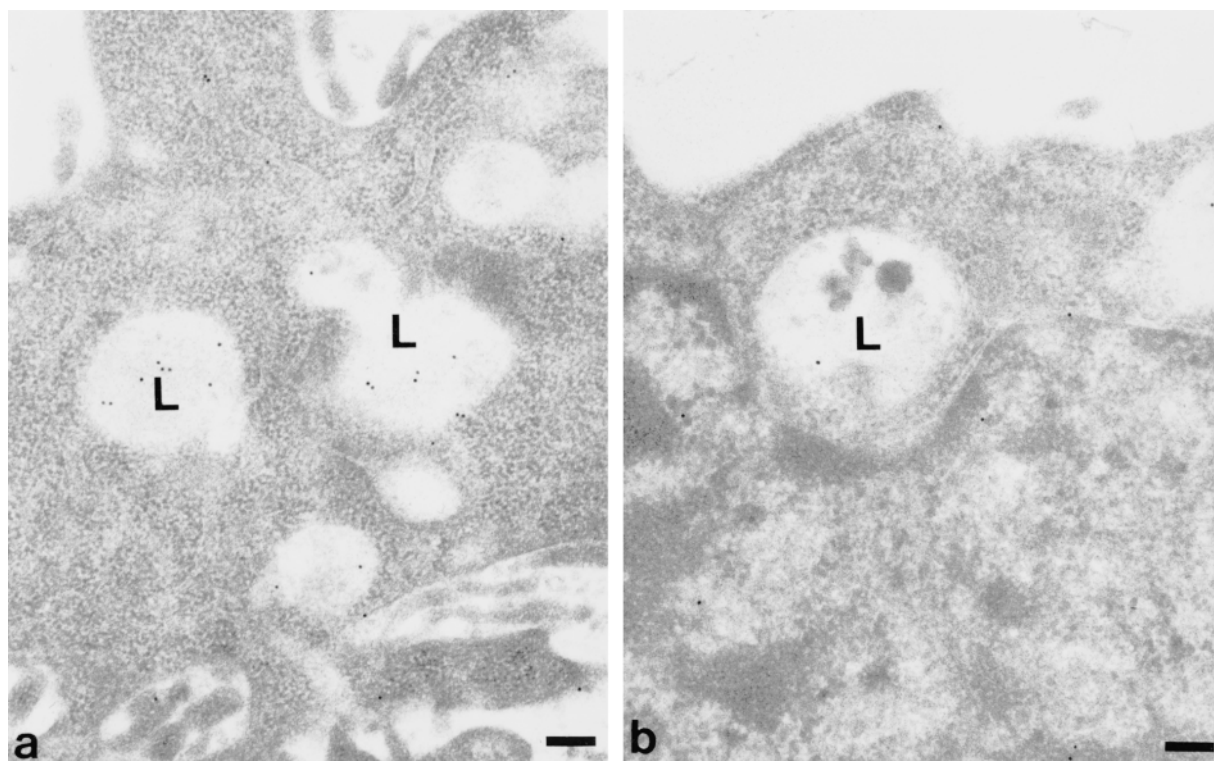


Fig. 3. a) CHO cell grown in control media. Note lysosome (L) moderately labeled with anti-prosaposin antibody; $\times 44,250$; bar 100 nm. b) CHO cell treated for 48 h with fumonisin B1 and labeled with anti-prosaposin antibody. Notice lysosome (L) unlabeled; $\times 34,000$; bar = 150 nm.

Tris-HCl-buffered saline (TBS) containing 15% (v/v) goat serum and then incubated for 30 min on a drop of anti-prosaposin antibody diluted 1:50 in TBS. The sections were then washed four times, for 5 min each time, in TBS containing 0.05% Tween-20. They were then transferred, for 15 min, to drops of TBS containing 15% goat serum, and incubated for 30 min on drops of colloidal gold (8–10 nm)-conjugated goat anti-rabbit IgG (Cedarlane, Hornby, Ontario, Canada). The sections were

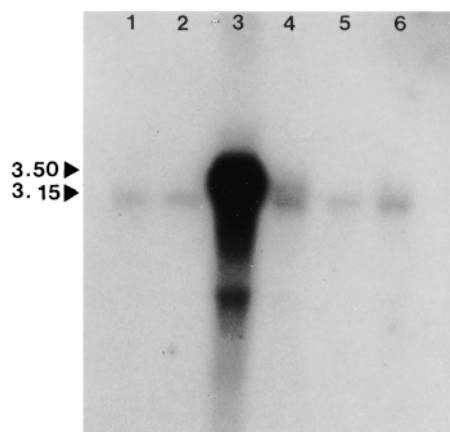


Fig. 4. Northern blot analysis of prosaposin mRNA in amplified cell lines. Total RNA (5 μg) isolated from 6 transformants resistant to 0.065 μM methotrexate was electrophoresed on an agarose gel, transferred to nylon, and hybridized to a prosaposin-DIG cDNA probe. Lanes 3 and 4 (designated clones 66 and 62, respectively) exhibit the presence of the bicistronic mRNA containing both endogenous prosaposin (3.15 kb) and prosaposin/dihydrofolate reductase sequence (3.50 kb).

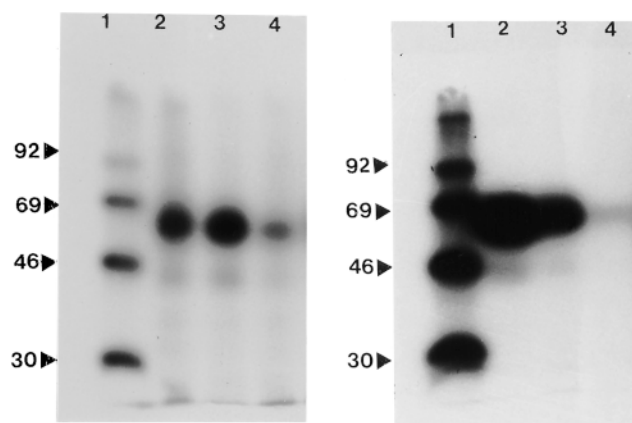


Fig. 5. Immunoprecipitation of prosaposin expressed in stably transformed CHO cells (clone 66) and control CHO cells. Control CHO (clone 74) cells were transformed with the vector p91093b without prosaposin cDNA and selected for resistance up to 0.5 μM of methotrexate. In both cases CHO cells were metabolically labeled with [^{35}S]methionine for 90 min. The labeled proteins were immunoprecipitated using anti-prosaposin antibody and separated by SDS-PAGE (10%) under reducing conditions. Radiolabeled bands, along with [^{14}C]methylated protein markers used as molecular standards, were visualized by fluorography. Left panel: lane 1, standards; lane 2, cell lysate of clone 66 treated with 0.12 μM methotrexate; lane 3, cell lysate of clone 66 treated with 0.24 μM methotrexate; lane 4, cell lysate of control CHO cells (clone 74) treated with 0.5 μM methotrexate. Right panel: lane 1, standards; lane 2, culture media of clone 66 treated with 0.12 μM methotrexate; lane 3, culture media of clone 66 treated with 0.24 μM methotrexate; lane 4, culture media of control CHO cells (clone 74) treated with 0.5 μM methotrexate. Note that fluorography revealed proteins corresponding to apparent molecular masses of 65 kDa in cell lysates and 70 kDa found in culture media.

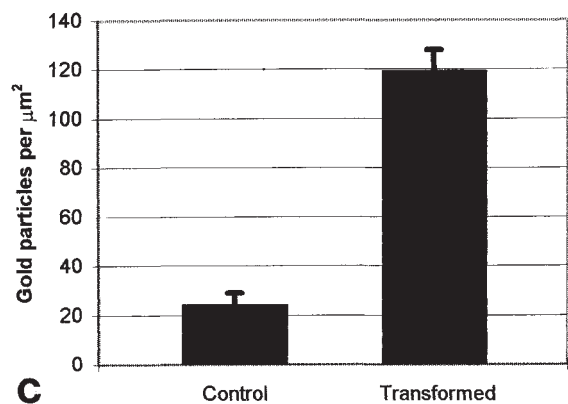
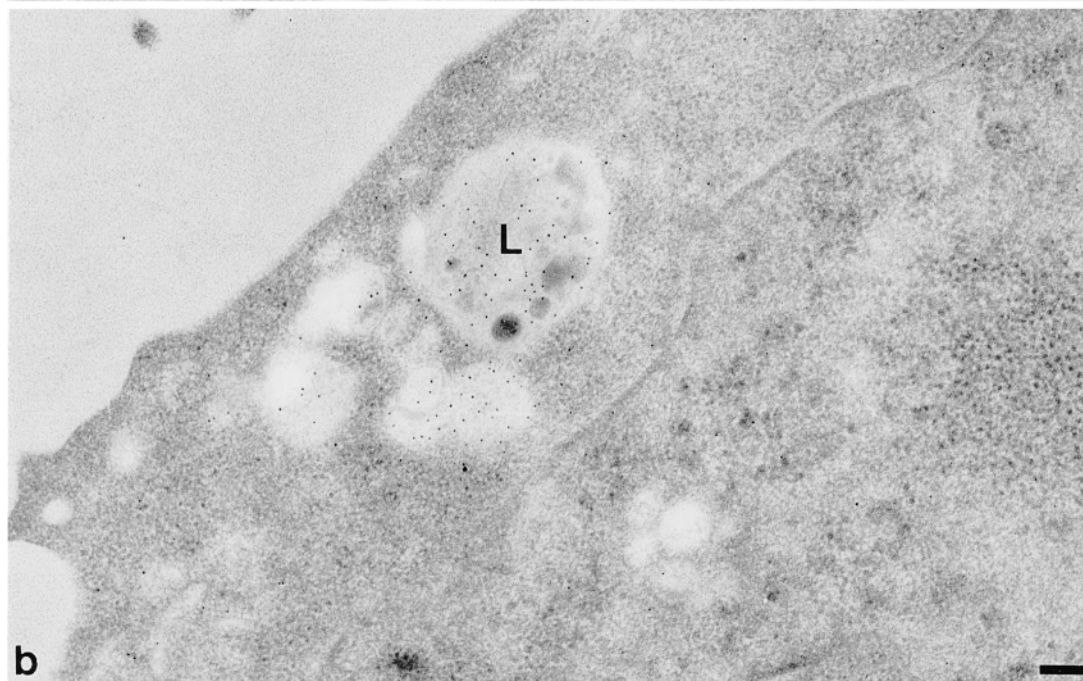
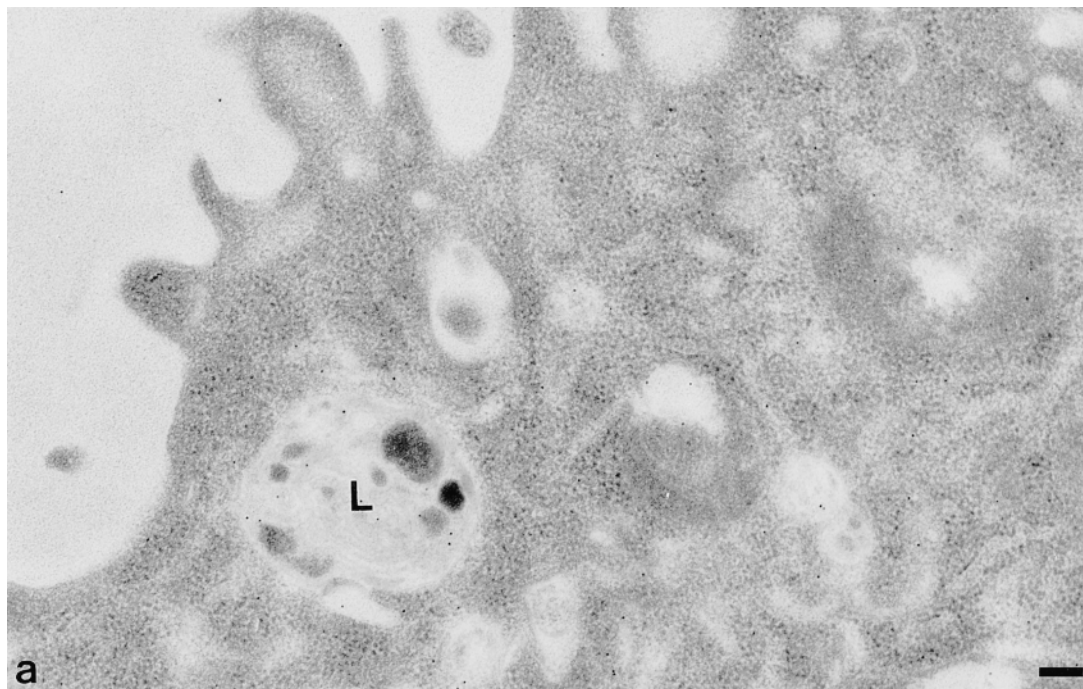


Fig. 6. Immunogold labeling with anti-prosaposin antibody of CHO cells transfected with the expression vector carrying (clone 66) or not (clone 74) the human prosaposin cDNA. a) Lysosome (L) of control CHO cell (clone 74) showing weak labeling. b) Lysosome (L) of clone 66 cell showing intense gold labeling. Magnification: $\times 30,000$; bar = 160. c) Bar graph representing the number of colloidal gold particles per μm^2 of lysosomes of CHO cells transfected with the expression vector carrying (clone 66) or not (clone 74) the prosaposin cDNA. Error bars represent standard deviation of the mean.

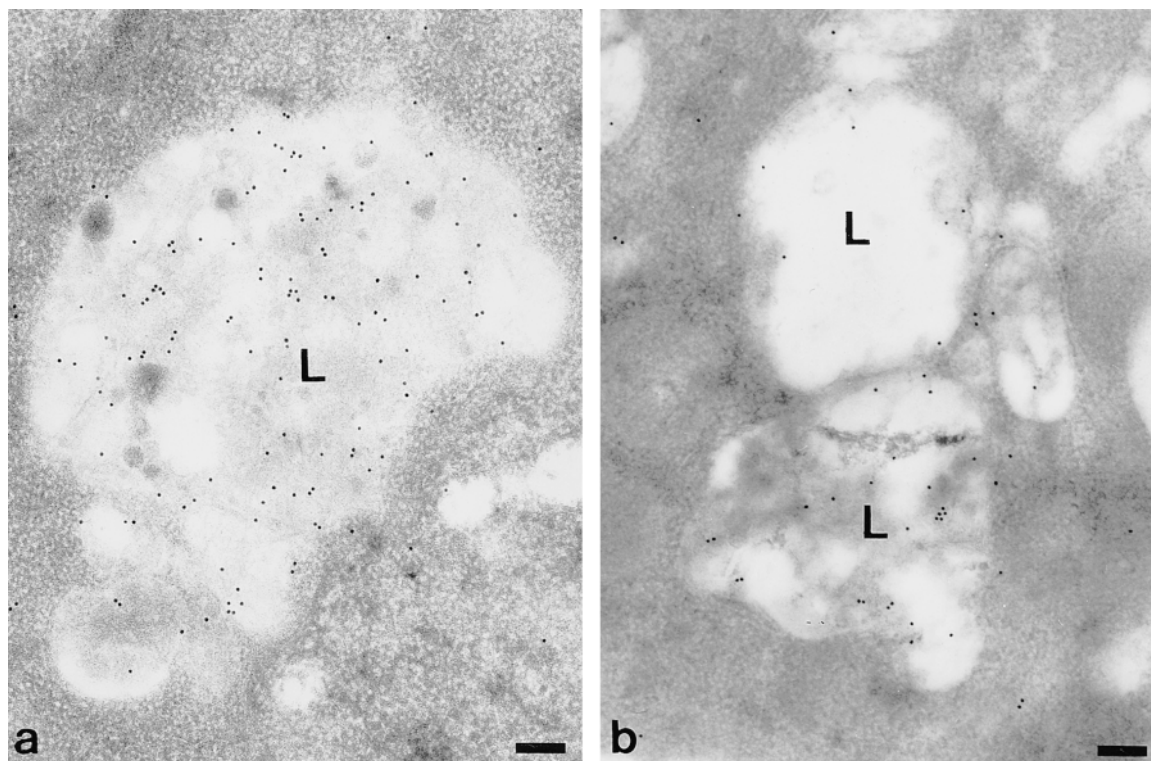


Fig. 7. a) CHO (clone 66) grown in media without fumonisin B1. Large lysosome (L) heavily labeled with anti-saposin A antibody; $\times 34,000$; bar = 160 nm. b) CHO (clone 66) cell treated with fumonisin B1 for 48 h. Two large lysosome (L) moderately labeled with anti-saposin A antibody; $\times 34,000$; bar = 160 nm.

then subjected to three 5-min washes in TBS containing 0.05% Tween-20 followed by two 5-min washes in distilled water. Sections were counterstained with uranyl acetate in 30% ethanol (2 min) followed by lead citrate (0.5 min). Normal rabbit serum served as control. Electron micrographs were taken on a Philips 400 electron microscope (Philips Electronics, Toronto, Ontario). Anti-prosaposin antibody was kindly donated by Dr. M. Griswold (Department of Biochemistry, Washington State University). The specificity of the antibody was tested on immunoblots of rat lysosomal proteins (20). Anti-cathepsin A and L antibodies were used as specific markers for lysosomes. The specificity of these antibodies were tested immunocytochemically (31, 32).

Quantitative electron microscopy

A quantitative analysis was performed on the lysosomes and small vesicles ($\geq 0.1 \mu\text{m}$ in diameter) were found around the Golgi apparatus of the different cell lines. One hundred cells per grid, containing 3 to 10 lysosomes, were chosen at random and photographed. Micrographs were taken at a magnification of $\times 25,000$. Profile areas of lysosomes and vesicles were measured with a Zeiss MOP-3 image analyzer (Carl Zeiss, Inc., Montreal, QC). The immunogold labeling density was obtained by averaging the mean values collected from three grids and expressed as number of gold particles per μm^2 .

RESULTS

Lysosomal markers

Anti-cathepsin A and L antibodies are specific markers for the lysosomal compartment and were used to identify

lysosomes in Lowicryl-embedded cells (**Fig. 1a**). Both antibodies labeled membrane bound structures of more than $0.2 \mu\text{m}$ in diameter showing various degrees of electron density. These structures were considered as lysosomes. Electron-lucent vesicles, less than $0.1 \mu\text{m}$ in diameter, found around or near the Golgi apparatus were unlabeled and were identified as secretory vesicles.

Effect of fumonisin B1 in NRK and CHO cells

Quantitative analysis of electron micrographs taken from NRK cells reacted with anti-prosaposin antibody demonstrated a decrease in density of colloidal gold labeling of 59% in the lysosomes of fumonisin B1-treated cells as compared to the non-treated NRK cells (Figs. 1b, 1c and **Fig. 2**). Chinese hamster ovary (CHO) cells showed a low level of expression of prosaposin. Fumonisin B1 treatment reduced the density of gold labeling with anti-prosaposin antibody by 85%, compared to the non-treated cells (**Figs. 3a, 3b, and Fig. 2**).

Selection of stably transformed of CHO cells

A major problem during the course of this investigation was the low level of expression of prosaposin in culture cells. Thus, in order to better define the role of GSLs in the transport of prosaposin, CHO cells were transformed with an expression vector containing a human prosaposin cDNA, followed by the dihydrofolate reductase sequence.

Northern blot analysis of transfected clones selected with $0.065 \mu\text{M}$ methotrexate demonstrated that two of them,

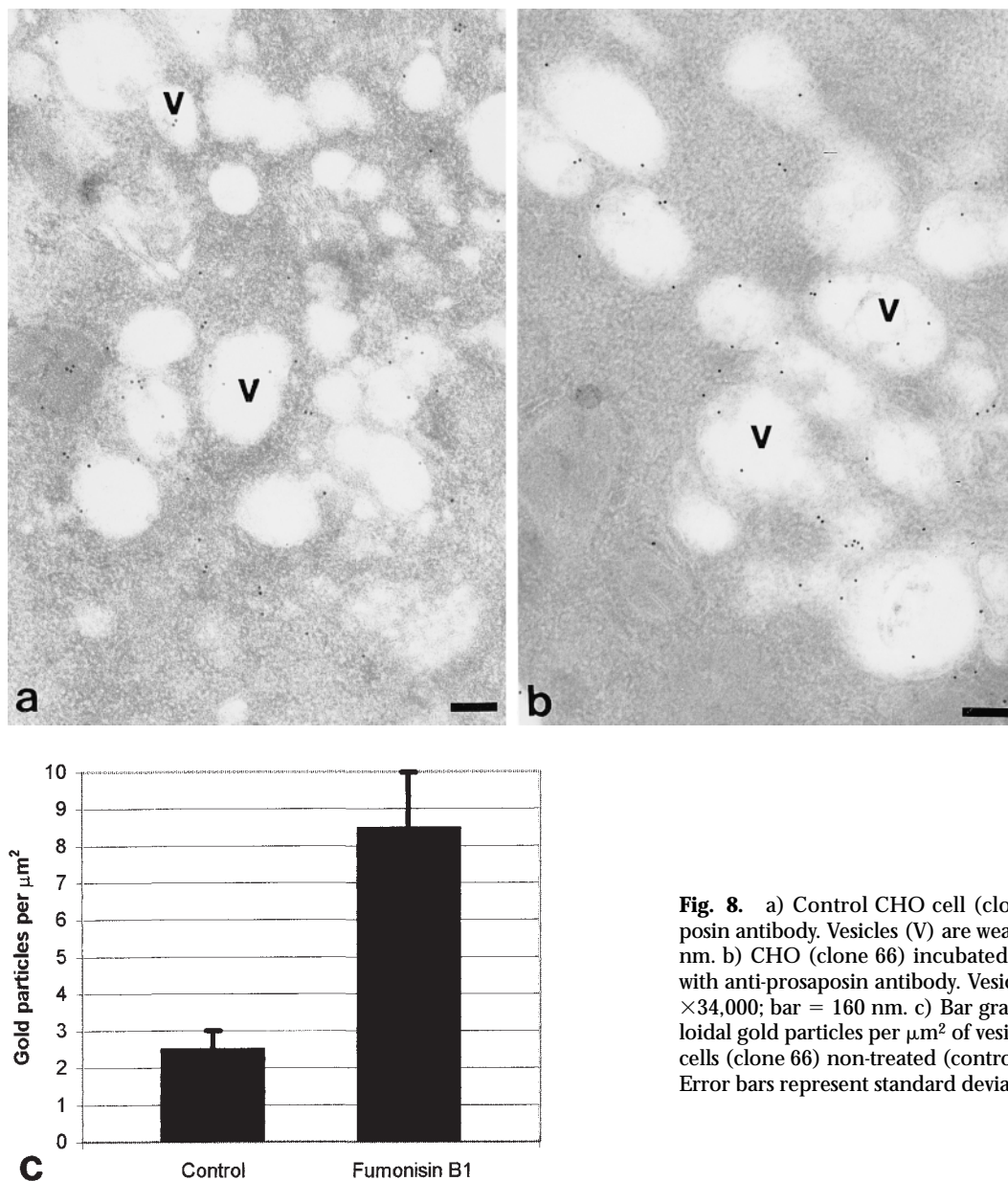


Fig. 8. a) Control CHO cell (clone 66) labeled with anti-prosaposin antibody. Vesicles (V) are weakly labeled; $\times 34,000$; bar = 160 nm. b) CHO (clone 66) incubated with fumonisin B1 and labeled with anti-prosaposin antibody. Vesicles (V) are moderately labeled; $\times 34,000$; bar = 160 nm. c) Bar graph representing number of colloidal gold particles per μm^2 of vesicles in the Golgi region of CHO cells (clone 66) non-treated (control) or treated with fumonisin B1. Error bars represent standard deviation of the mean.

designated clones 66 and 62, exhibit the presence of bicistronic mRNAs containing both endogenous prosaposin (3.15 kb) and prosaposin/dihydrofolate reductase sequence (3.50 kb), respectively (Fig. 4).

Because clone 66 produced larger quantities of prosaposin mRNA, it was tested for the production of prosaposin protein. Figure 5 shows two results from SDS polyacrylamide gel electrophoresis of immunoprecipitated prosaposin from stably transformed CHO cells (clone 66). Autoradiography revealed two labeled proteins corresponding to apparent molecular masses of 65 kDa found in cell lysates and 70 kDa found in culture media. The intensity of the labeled band of clone 66 was 4- to 7-fold higher than that of the control CHO cell line transfected with the same vector without the prosaposin cDNA (clone 74).

Immunogold labeling with anti-prosaposin antibody of CHO cells transfected with the expression vector carrying the human prosaposin cDNA (clone 66) showed in-

tense labeling of the lysosomes (Fig. 6a and b). When the number of colloidal gold particles per μm^2 of lysosomes was compared between clone 66 and clone 74 CHO cells (control), a 5-fold increase was found in the transformed cells (Fig. 6c). Sections of control CHO cells and of clone 66 CHO cells incubated with normal rabbit serum did not show any reactivity in the lysosomes (data not shown).

Effect of fumonisin B1 on stably transfected CHO cells (clone 66)

Overexpression of prosaposin caused a heavy labeling of the lysosomes of CHO cells (clone 66) with anti-prosaposin antibody. Fumonisin B1 treatment decreased the density of immunogold labeling by 55% in the lysosomes of these cells compared to the non-treated cells. (Fig. 2, and 7a and b). On the other hand, the gold particle density increased by 3-fold in the small vesicles (less than $0.1 \mu\text{m}$ in diameter) found around the nucleus or near the Golgi ap-

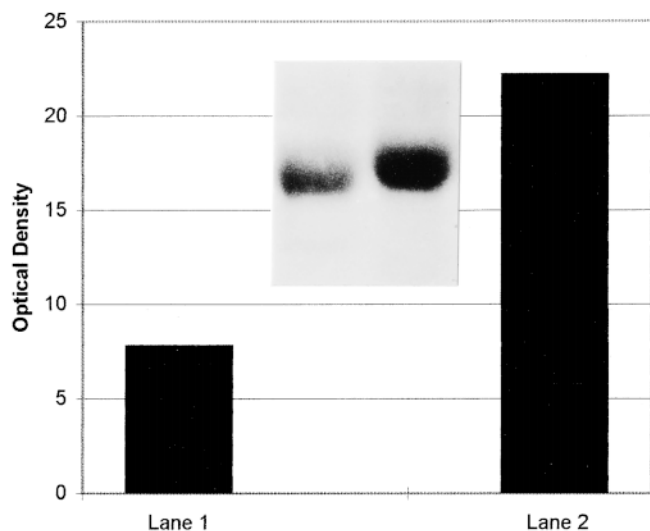


Fig. 9. Immunoblotting of culture media proteins from stably transformed CHO cells (clone 66) reacted with anti-prosaposin antibody. Culture media from clone 66 CHO cells untreated with fumonisin B1 contains a 70 kDa band (lane 1). This band is stronger in fumonisin B1-treated cells (lane 2). Densitometric analysis demonstrated a 3-fold increase of prosaposin in the media of fumonisin B1-treated cells.

paratus in fumonisin B1-treated cells compared to the non-treated cells (**Fig. 8a, b, and c**). A reduction in labeling of these vesicles was also found in the other cell lines treated with fumonisin B1 (data not shown).

Immunoblotting with anti-prosaposin antibody revealed that culture media from clone 66 CHO cells contained a major 70 kDa band and that this band was stronger in fumonisin B1-treated cells (**Fig. 9**).

Immunogold labeling studies with anti-cathepsin A antibody

Cathepsin A is a lysosomal hydrolase known to be targeted to the lysosomes via the mannose 6-phosphate receptor. In order to determine whether the mannose

6-phosphate receptor pathway was affected by the fumonisin B1 treatment, an anti-cathepsin A antibody was used. Quantitative immunoelectron microscopy using anti-cathepsin A antibody with NRK, CHO, and clone 66 CHO cells treated or not with fumonisin B1 showed no significant differences ($P \leq 0.05$) in the immunogold labeling density in the lysosomes (**Fig. 10**).

Confocal microscopy

Control untreated CHO cells (clone 66) showed an intense reaction with anti-prosaposin antibody in the perinuclear Golgi region. A granular reaction was also observed on the periphery of this region which appears to correspond to stained lysosomes. Fumonisin B1 treatment produced a loss of granular staining and a slight decrease in Golgi fluorescence. PDMP-treated cells displayed a pattern similar to the untreated control cells. Finally, D609-treated cells did not display any immunoreactivity (**Fig. 11**).

DISCUSSION

Protein targeting to the lysosomes most commonly occurs via the mannose 6-phosphate receptor which directs soluble hydrolases from the Golgi apparatus to the lysosomes (3). Transmembrane lysosomal proteins are transported by an alternative pathway from the Golgi apparatus to the plasma membrane and then to the lysosomes via endocytosis (4–6).

Prosaposin exists as a 70 kDa protein that is secreted to the extracellular space and a 65 kDa intracellular protein that is routed to the lysosomes (20). Although lysosomal prosaposin is not a transmembrane protein, biochemical studies showed that this molecule is associated with Golgi membranes (33) and that it may bind sphingolipids (2). Nevertheless, the mechanism of transport of prosaposin to the lysosomes is still unknown. Thus, we decided to test the hypothesis that prosaposin is transported from the Golgi apparatus to the lysosomes bound to sphingolipids anchored to the membrane of cargo vesicles.

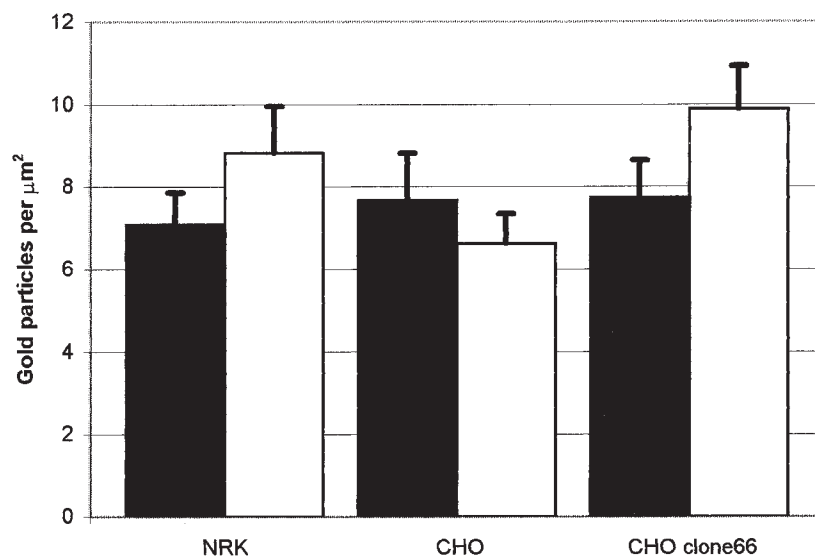


Fig. 10. Bar graph showing immunogold labeling density of cathepsin A antibody in lysosomes of cell lines treated or not with fumonisin B1. Treatment with fumonisin B1 did not cause any significant difference in the labeling density. Error bars represent standard deviation of the mean.

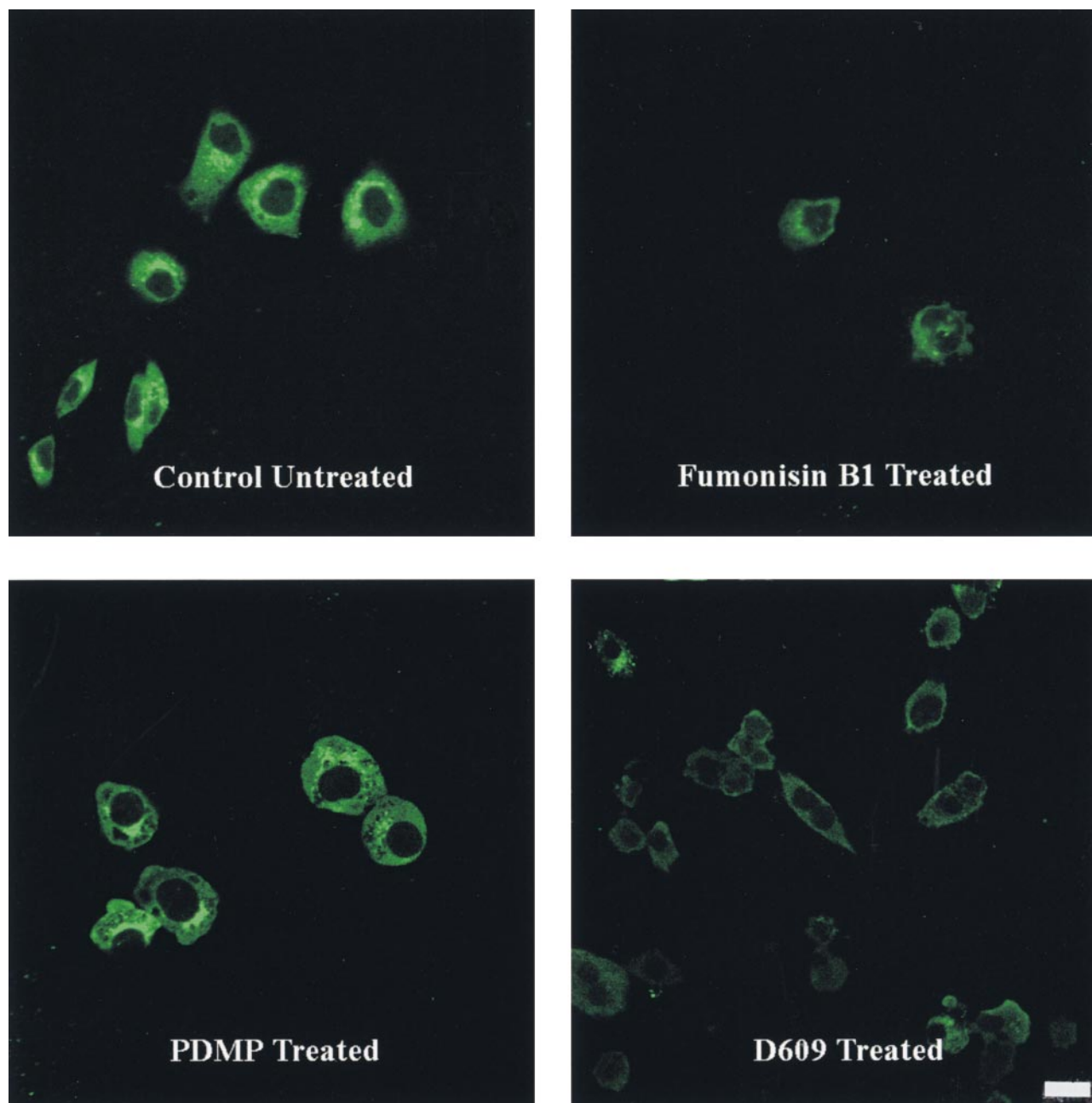


Fig. 11. Confocal microscopy of cells immunostained with anti-prosaposin antibody. Control untreated CHO cells (clone 66) shows a granular reaction in the Golgi region of these cells. Fumonisin B1 abolished the granular staining. PDMP treatment did not cause any change in the staining pattern. D609 incubation abolished both Golgi and granular staining; $\times 600$; bar = 10 μm .

To examine this hypothesis, the synthesis of glycosphingolipids and sphingomyelin was selectively inhibited with fumonisin B1, a fungal metabolite that blocks the formation of ceramide, and with chemical compounds such as PDMP and D609, which inhibit the synthesis of glucosyl-ceramide and sphingomyelin, respectively (34) (Fig. 12).

Fumonisin B1 decreased the immunogold labeling of lysosomes with anti-prosaposin antibody, although the range of variation was relatively wide. This was attributed to different responses to fumonisin B1 by the various cell types used in this investigation. Total inhibition was never

achieved, possibly, due to the presence of endogenous sphingolipids.

A major problem in assessing the labeling of prosaposin in lysosomes was the weak immunoreactivity of cultured cells. To overcome this problem, CHO cells were stably transfected with an expression vector containing a human prosaposin cDNA. Overexpression of lysosomal and secreted prosaposins were found in two positive clones. A clone designated 66 was selected for this study. Fumonisin B1 produced a 55% reduction in the lysosomes and a 3-fold increase in small vesicles found around the Golgi apparatus of these cells. The small vesicles were considered

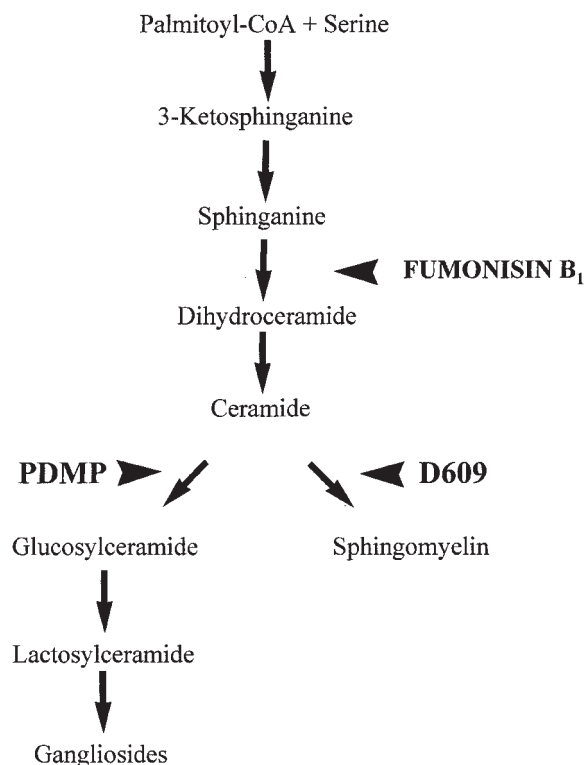


Fig. 12. Biosynthesis of glycosphingolipids and sphingomyelin. The inhibitors used in this study are shown in bold and their site action is indicated by arrowheads.

to be secretory elements due to their small size, their association with the Golgi apparatus, and their lack of reactivity with anti-cathepsin L antibody.

These results indicated that fumonisin B1 blocked the transport of prosaposin to the lysosomes, perhaps redirecting the protein to the secretory pathway. To verify that this was the case, culture media of cells treated or not with fumonisin B1 were collected and examined by immunoblotting. The samples were taken from replica plates grown to confluency. Equivalent amounts of protein loaded onto a SDS-PAGE gel revealed that fumonisin B1 induced the release of the 70 kDa (secretory form) prosaposin into the media.

A recent investigation suggested that prosaposin reaches the lysosomes by a mechanism of secretion and endocytosis in I-cell disease fibroblasts (21). Nonciliated cells of the efferent ducts have also been shown to internalize prosaposin dissociated from spermatozoa (32), but this process was linked to a mechanism of clearance rather than to a process of targeting of prosaposin to the lysosomes. However, investigations carried out in our laboratory indicated that prosaposin is transported to lysosomes directly from the Golgi apparatus (20, 33).

Prosaposin was initially found to be targeted to lysosomes by a mannose 6-phosphate-independent pathway in various cell types (18, 21, 33). Tunicamycin failed to impair the targeting of prosaposin to the lysosomes (33). When Golgi subcellular fractions from Sertoli cells were permeabilized with mild detergents, the 70 kDa secreted form of prosaposin was released but the 65 kDa lysosomal

form of this protein was retained. Similarly, when permeabilized Golgi fractions were incubated in excess of free mannose 6-phosphate, the 65 kDa protein remained associated to Golgi membranes (33). Metabolic labeling of Sertoli cells demonstrated that prosaposin is first synthesized as a 65 kDa form which is post-translationally modified to a 70 kDa polypeptide that is secreted to the extracellular space. A fraction of the 65 kDa form is targeted to the lysosomes where it is cleaved into 15 kDa proteins (20). Finally, lysosomal subcellular fractions only contain the 65 kDa form of prosaposin (20). This evidence demonstrates that the 65 kDa protein but not the 70 kDa extracellular form of prosaposin is the precursor of the lysosomal saposins. Secreted prosaposin was found in various fluids such as milk (35), seminiferous tubular fluid (20), cerebrospinal fluid, bile, and pancreatic juice (36), but its function in extracellular compartments is still unknown.

In order to examine whether the mannose 6-phosphate receptor pathway was affected by fumonisin B1, treated and non-treated cells were reacted with an anti-cathepsin A antibody. Cathepsin A is a soluble lysosomal hydrolase that is targeted to the lysosomal compartment via the mannose 6-phosphate receptor system (37). Quantitative immunoelectron microscopy of NRK, CHO, and CHO clone 66 cell lines, treated or not with fumonisin B1, showed no significant differences in the immunogold labeling density with the anti-cathepsin A antibody. This result indicated that fumonisin B1 has no effect on the transport of cathepsin A, and that the effect on the targeting of prosaposin was specific.

Immunofluorescence confocal microscopy confirmed the immunogold labeling results. Fumonisin B1-treated cells lost the granular fluorescence, indicating that the transport of prosaposin to the lysosomes was blocked. As fumonisin B1 inhibits the synthesis of both glycosphingolipids and sphingomyelin, two more specific inhibitors were used in this study. PDMP, which inhibits the formation of glycosphingolipids, had no effect on the fluorescent label of treated cells. On the other hand, D609, which affects the synthesis of sphingomyelin, abolished the fluorescent staining of treated cells. These findings suggest that sphingomyelin appears to be the sphingolipid implicated in the transport of prosaposin to the lysosomes.

Alternatively, the abolition of immunoreactivity by fumonisin B1 and D609 could be attributed to a nonspecific inhibition of prosaposin synthesis. This scenario appears to be unlikely, at least in the case of fumonisin B1-treated cells, which continue to produce and secrete more prosaposin in the media (Fig. 9).

In conclusion, our data support the hypothesis that sphingolipids may be involved in the transport of the 65 kDa form of prosaposin to the lysosomal compartment. This study also raises the question as to whether or not other lysosomal activators of sphingolipid degradation utilize a similar mechanism of transport to the lysosomes. **■**

Supported by MRC to C. R. M. and M. P. Carlos R. Morales is a Fellow from FRSQ.

Manuscript received 16 October 1998 and in revised form 31 March 1999.

REFERENCES

- Sandhoff, K., and T. Kolter. 1996. Topology of glycosphingolipid degradation. *Trends Cell Biol.* **6**: 98–103.
- Hiraiwa, M., S. Soeda, Y. Kishimoto, and J. S. O'Brien. 1992. Binding and transport of gangliosides by prosaposin. *Proc. Natl. Acad. Sci. USA.* **89**: 11254–11258.
- Kornfeld, R., and S. Kornfeld. 1985. Assembly of asparagine-linked oligosaccharides. *Annu. Rev. Biochem.* **54**: 631–664.
- Rohrer, J., A. Schweizer, D. Russell, and S. Kornfeld. 1996. The targeting of Lamp1 to lysosomes is dependent on the spacing of its cytoplasmic tail tyrosine sorting motif relative to the membrane. *J. Cell Biol.* **132**: 565–576.
- Braun, M., A. Waheed, and K. von Figura. 1989. Lysosomal acid phosphatase is transported to lysosomes via the cell surface. *EMBO J.* **8**: 3633–3640.
- Fambrough, D. M., K. Takeyasu, J. Lippencott-Schwarz, and N. R. Siegel. 1988. Structure of LEP100, a glycoprotein that shuttles between lysosomes and the plasma membrane, deduced from the nucleotide sequence of the encoding cDNA. *J. Cell Biol.* **106**: 61–67.
- Reitman, M. L., and S. Kornfeld. 1981. Lysosomal targeting, N-acetylglucosylphosphotransferase selectively phosphorylates native lysosomal enzymes. *J. Biol. Chem.* **256**: 11977–11980.
- Varki, A., and S. Kornfeld. 1981. Purification and characterization of rat liver α -N-acetylglucosaminyl phosphodiesterase. *J. Biol. Chem.* **256**: 9937–9943.
- Waheed, A., A. Hasilik, and K. von Figura. 1981. Processing of the phosphorylated recognition marker in lysosomal enzymes. Characterization and partial purification of a microsomal α -N-acetylglucosaminyl phosphodiesterase. *J. Biol. Chem.* **256**: 5717–5721.
- Goldberg, D. E., and S. Kornfeld. 1983. Evidence for extensive subcellular organization of an asparagine-linked oligosaccharide processing and lysosomal enzyme phosphorylation. *J. Biol. Chem.* **258**: 3159–3165.
- Brown, W. J., J. Goodhouse, and M. G. Farquhar. 1986. Mannose-6-phosphate receptors for lysosomal enzymes cycle between the Golgi complex and endosomes. *J. Cell Biol.* **103**: 1235–1247.
- Pohlmann, R., C. Krentler, B. Schmidt, W. Schroder, G. Lorkowski, J. Cully, G. Mersmann, C. Geier, A. Waheed, S. Gottschalk, H. Grzeschik, A. Hasilik, and K. von Figura. 1988. Human lysosomal acid phosphatase: cloning, expression and chromosomal assignment. *EMBO J.* **7**: 2343–2350.
- Waheed, A., S. Gottschalk, A. Hille, C. Krentler, R. Pohlmann, T. Braulke, H. Hauser, H. Geuze, and K. von Figura. 1988. Human lysosomal acid phosphatase is transported as a trans membrane protein to lysosomes in transfected baby hamster kidney cells. *EMBO J.* **7**: 2351–2358.
- Peters, C., M. Braun, B. Weber, M. Wendland, B. Schmidt, R. Pohlmann, A. Waheed, and K. von Figura. 1990. Targeting of a lysosomal membrane protein: a tyrosine-containing endocytosis signal in the cytoplasmic tail of lysosomal acid phosphatase is necessary and sufficient for targeting to lysosomes. *EMBO J.* **9**: 3497–3506.
- Pearse, B. M. F. 1988. Receptors compete for adaptors found in plasma membrane coated pits. *EMBO J.* **7**: 3331–3336.
- Glickman, J. N., E. Conibear, and B. M. F. Pearse. 1989. Specificity of binding of clathrin adaptors to signals on the mannose-6-phosphate/insulin-like growth factor II receptor. *EMBO J.* **8**: 1041–1047.
- Ogata, S., and M. Fukuda. 1994. Lysosomal targeting of Limp II membrane glycoprotein requires a novel Leu-Ile motif at a particular position in its cytoplasmic tail. *J. Biol. Chem.* **269**: 5210–5217.
- Rijnboutt, S., H. M. F. G. Aerts, H. J. Geuze, J. Targer, G. J. Strouss. 1991. Mannose 6-phosphate-independent membrane association of cathepsin D, glucocerebroside and sphingolipid-activating protein. *J. Biol. Chem.* **266**: 4862–4868.
- Zhu, Y., and G. E. Conner. 1994. Intermediate association of lysosomal protein precursors during biosynthesis. *J. Biol. Chem.* **269**: 3846–3851.
- Igdoura, S. A., and C. R. Morales. 1995. Role of sulfated glycoprotein-1 (SGP-1) in the disposal of residual bodies by Sertoli cells of the rat. *Mol. Reprod. Dev.* **40**: 91–102.
- Vielhaber, G., R. Hurwitz, and K. Sandhoff. 1996. Biosynthesis, processing and targeting of sphingolipid activator protein (SAP) precursor in cultured human fibroblasts. *J. Biol. Chem.* **271**: 32435–32446.
- Morimoto, S., M. B. Martin, Y. Yamamoto, K. A. Kretz, and J. S. O'Brien. 1989. Saposin A: second cerebroside activator protein. *Proc. Natl. Acad. Sci. USA.* **86**: 3389–3393.
- Murray, M. J., R. J. Kaufman, S. A. Latt, and R. A. Weinberg. 1983. Construction and use of a dominant, selectable marker: a Harvey sarcoma virus-dihydrofolate reductase chimera. *Mol. Cell. Biol.* **3**: 32–43.
- Zhao Q., A. W. Bell, M. El-Alfy and C. R. Morales. 1998. Mouse testicular sulfated Glycoprotein-1: sequence analysis of the common backbone structure of prosaposins. *J. Androl.* **19**: 165–174.
- Morales, C. R., N. Hay, M. El-Alfy and Q. Zhao. 1998. Distribution of mouse sulfated glycoprotein-1 (prosaposin) in the testis and other tissues. *J. Androl.* **19**: 156–164.
- Maniatis, T., E. F. Fritsch, and J. Sambrook. (eds) 1982. Molecular Cloning; a Laboratory Manual. Cold Spring Harbor, New York.
- Laemmli, E. K. 1970. Cleavage of structural proteins during the assembly of the head of the bacteriophage T4. *Nature.* **227**: 680–685.
- Khyse-Anderson, J. 1984. Electrophoretic transfer of multiple gels: a simple apparatus without buffer tank for rapid transfer of proteins from polyacrylamide to nitrocellulose. *J. Biochem. Biophys. Methods.* **10**: 203–209.
- Sylvester, S. R., C. R. Morales, R. Oko, and M. D. Griswold. 1989. Sulfated glycoprotein-1 (saposin precursor) in the reproductive system of the male rat. *Biol. Reprod.* **41**: 941–948.
- Hermo, L., J. Wright, R. Oko, and C. R. Morales. 1991. Role of epithelial cells of the male excurrent duct system of the rat in the endocytosis or secretion of sulfated glycoprotein-2 (clusterin). *Biol. Reprod.* **44**: 1113–1131.
- Satake, A., K. Itoh, M. Shimimoto, T. C. Saido, H. Sakuraba, and Y. Suzuki. 1994. Distribution of lysosomal protective protein in human tissues. *Biochem. Biophys. Res. Commun.* **205**: 38–43.
- Igdoura, S. A., C. R. Morales, and L. Hermo. 1995. Differential expression of cathepsins B and D in testis and epididymis of adult rats. *J. Histochem. Cytochem.* **43**: 545–557.
- Igdoura, S. A., A. Rasky, and C. R. Morales. 1996. Trafficking of sulfated glycoprotein-1 (prosaposin) to lysosomes or to the extracellular space in rat Sertoli cells. *Cell Tissue Res.* **283**: 385–394.
- Mays, R. W., K. A. Stemers, B. A. Fritz, A. W. Lowe, G. van Meer, and J. W. Nelson. 1995. Hierarchy of the mechanism involved in generating Na/K ATPase polarity in MDCK epithelial cells. *J. Cell Biol.* **130**: 1105–1116.
- Kondoh, K., Y. Hineno, A. Sano, and Y. Kakimoto. 1991. Isolation and characterization of prosaposin from human milk. *Biochem. Biophys. Res. Commun.* **181**: 286–292.
- Hineno, T., A. Sano, K. Kondoh, S. Veno, Y. Kakimoto, and K. Yoshida. 1991. Secretion of sphingolipid hydrolase activator precursor, prosaposin. *Biochem. Biophys. Res. Commun.* **176**: 668–674.
- Sleat, D. E., I. Sohar, H. Lackland, J. Majercak, and P. Lobel. 1996. Rat brain contains high levels of mannose-6-phosphorylated glycoproteins including lysosomal enzymes and palmitoyl-protein thioesterase, an enzyme implicated in infantile neuronal lipofuscinosis. *J. Biol. Chem.* **271**: 19191–19198.